BeFo
STIFTELSEN BERGTEKNISK FORSKNING
ROCK ENGINEERING RESEARCH FOUNDATION

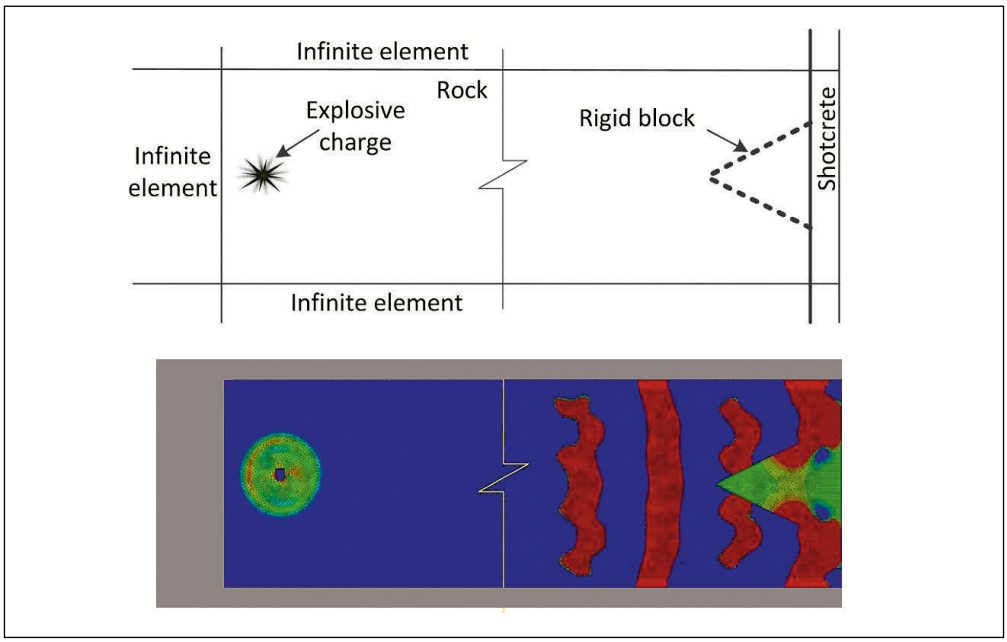

FAILURE MODES OF SHOTCRETE ON JOINTED ROCK SUBJECTED TO IMPACT-TYPE LOADS

Lamis Ahmed

Grundvattennivåer, pH och sulfatkoncentrationer i bergborrhål BP08 (Figur 12 i rapporten).

STIFTELSEN BERGTEKNISK FORSKNING
ROCK ENGINEERING RESEARCH FOUNDATION

Failure modes of shotcrete on jointed rock subjected to impact-type loads

Brottmoder hos sprutbetong på sprucket berg utsatt för sprängning eller vibrationer av stöttyp

Lamis Ahmed, KTH

BeFo Report 166
Stockholm 2016
ISSN 1104 – 1773
ISRN BEFO-R—166—SE

Preface

Shotcrete is concrete projected pneumatically onto a surface, using either the dry mix or the wet mix method. The latter has been widely used for tunnelling work in hard rock and its flexibility in the choice of application thickness, material compositions (e.g., fibre content), output capacity and quick early strength development makes shotcrete a material well suited for rock support. Most construction work underground in rock involves the use of explosives for excavation work. Rock surfaces are often secured with shotcrete immediately after the excavation blasting to prevent fallout of smaller blocks. Therefore, shotcrete must often be able to carry loads and withstand disturbances early after spraying.

To improve the understanding of how vibrations affect hardened shotcrete, finite element analyses were carried out. The numerical model was used to calculate load cases of the shotcrete on fractured rock walls subjected to blasting with delay time.

The work presented in this report was carried out at the KTH Royal Institute of Technology, Division of Concrete Structures by Lamis Ahmed. The study was made possible through financial support from BeFo (Rock Engineering Research Foundation). The researcher was supported by an advisory group consisting of Anders Ansell and Richard Malm from KTH. Evaluation and presentation of the results were carried out jointly by the researcher and support from a reference group consisting of Johan Silfwerbrand (KTH), Thomas Dalmalm (Swedish Transport Administration), Hans-Åke Mattsson (ÅF), Ulf Nyberg (LTU), Fredrik Johansson (KTH/SWECO) and Per Tengborg (BeFo).

Stockholm
Per Tengborg

Förord

Sprutbetong är betong som appliceras pneumatiskt på en bergyta, antingen som torr- eller våt sprutad. Den senare har använts i stor utsträckning för tunnelarbete i berg och dess flexibilitet avseende tjocklek, materialsammansättningar (t.ex. fiberinnehåll), produktionskapacitet och tidig hållfasthetutveckling gör sprutbetong till ett material väl lämpat för bergförstärkning. De flesta underjordiska byggnadsarbeten innebär användning av sprängämnen och bergytor säkras ofta med sprutbetong direkt efter sprängning för att förhindra nedfall av mindre block. Därför måste sprutbetong ofta kunna bära laster och motstå vibrationer redan tidigt efter applicering.

För att förbättra förståelsen för hur vibrationer påverkar hårdnad sprutbetong har finita elementanalyser genomfört. Den numeriska modellen användes för att analysera några olika lastfall för sprutbetong på bergväggar som utsätts för vibrationen från sprängning med fördröjning.

Arbetet som presenteras i denna rapport genomfördes vid Kungliga Tekniska Högskolan (KTH), avdelningen för Betongkonstruktion av Lamis Ahmed. Studien har gjorts möjlig genom ekonomiskt stöd från BeFo (Stiftelsen Bergteknisk Forskning). Forskaren stöddes av en rådgivande grupp bestående av Anders Ansell och Richard Malm från KTH. Utvärdering och presentation av resultaten har genomförts gemensamt av forskargruppen som till stöd har haft en referensgrupp bestående av Johan Silfwerbrand (KTH), Thomas Dalmalm (Trafikverket), Hans-Åke Mattsson (ÅF), Ulf Nyberg (LTU), Fredrik Johansson (KTH/SWECO) och Per Tengborg (BeFo).

Stockholm
Per Tengborg

Abstract

Rock support is usually designed for static loading conditions, but most construction work in underground rock involves the use of explosives for excavation work. Thus the tunnels are also subjected to dynamic loads. The detonation of explosives during excavations of tunnels and underground spaces lead to stress waves that propagate through the rock and may cause severe damage to shotcrete in, e.g. a neighbouring tunnel. It is concluded from previous investigations that shotcrete can withstand high particle velocity vibrations without being seriously damaged. Shotcrete without reinforcement can survive vibration levels as high as 500−1000 mm/s while loss of bonding and ejected rock will occur for vibration velocities higher than 1000 mm/s.

In this study, dynamic finite element models of rock and shotcrete subjected to stress waves have been developed using a finite element program. The models were evaluated and refined through comparisons between calculated and measured data. The simulations were performed using two-dimensional plane strain elements. The models describe several cases with respect to the position of the detonation point. The blast load is introduced in the model as an explosive material within the rock mass causing a vibrational energy after the detonation. Non-linear properties of the rock is introduced, making it possible to describe the detonation within the rock mass. To allow the stress wave to disperse, a relatively large volume of rock is modelled. The stresses that occur at the interface between the shotcrete and the rock, when the explosion occurs, are calculated with the purpose to demonstrate the variation of the stresses due to the delay time between two explosive charges.

Initially, the simulation of stress wave propagation through intact rock, from one explosive charge towards the shotcreted rock surface, has been performed. Then, the models are modified to include the effect of rock fractured due to contour blasting, where the charges are situated around the tunnel perimeter. The fractured rock is represented as a translating wedge, i.e. a single rigid body.

It is demonstrated that the numerical modelling adopted in this study is feasible, and allows predictions of the blasting vibration at the shotcrete-rock interface. The complex superposition of incident, reflected and transmitted stress waves at this interface can be illustrated by the results from the suggested numerical models.

Keywords: Shotcrete, Fractured rock, Vibration, Stress waves, Numerical analysis

Sammanfattning

Bergförstärkning är normalt anpassad för statiska belastningsförhållanden, men de flesta underjordiska byggnadsarbeten innebär användning av sprängämnen. Således är tunnlarna också utsätta för dynamisk belastning. Detonationen av sprängämnen vid konstruktion av tunnlar och underjordiska utrymmen leder till stötvågor som propagerar genom berget och kan orsaka allvarliga skador på sprutbetong i t.ex. en angränsande tunnel. Slutsatsen från tidigare undersökningar är att sprutbetong kan motstå vibrationsnivåer så höga som 500 till 1000 mm/s, vid högre vibrationshastigheter kan partier med förlorad vidhäftning till berget och utstötning.

I denna studie har dynamiska finita elementmodeller av berg och sprutbetong utsatta för stötvågor utvecklats med hjälp av ett finit elementprogram. Modellerna utvärderades och förfinades genom jämförelser mellan beräknade och uppmätta data. Simuleringarna utfördes med användning av två-dimensionella plana töjningselement. Modellerna beskriver flera fall avseende olika positionen för laddningar. Lasten från detonationen införs i modellen som ett sprängämne i bergmassan. Icke-linjära egenskaper för bergmaterial introduceras, vilket gör det möjligt att beskriva detonationen i bergmassan. En relativt stor volym berg modellerades för att tillåta stötvågen att dispergera. De spänningar som uppkommer vid gränsytan mellan sprutbetong och berget på grund av explosionen beräknas i syfte att demonstrera variationen av spänningar orsakade av fördröjningstiden mellan två sprängladdningar.

Initialt simulerades vågutbredning i intakt berg, från sprängämnesladdningen till sprutbetongen. Därefter modifierades modellerna för att innefatta effekten av bergsprickor runt tunnelns omkrets på grund av sprängning. Det uppspruckna berget representeras därmed som en bergskil, d.v.s. ett styvt block avgränsat av fördefinierade sprickor.

Det visar sig att de antagna förutsättningarna för modellerna är lämpliga, och gör det möjligt att förutsäga vibrationer från sprängning. Den komplexa överlagringen av infallande stötvågor, som reflekteras och transmitteras vid gränsytan, illustreras av resultaten från de föreslagna numeriska modellerna.

Nyckelord: Sprutbetong, Sprucket berg, Vibration, Spänningsvågor, Numerisk analys

Contents

Chapter 1

Introduction

In underground construction and tunnelling, the strive for a more time-efficient construction process naturally focuses on the possibilities of reducing the times of waiting between stages of construction. However, to assess the operational security and structural safety needs of the underground transportation infrastructure, there is a need to develop guidelines and recommendations to improve the security of the existing underground transportation infrastructure and facilities.

1.1 Background

The performance of shotcrete exposed to high magnitudes of vibration was investigated by Ahmed (2015) to identify safe distances for underground and tunnelling construction, using numerical analyses and comparison with measurements and observations. In the doctorate study, simulation of stress wave propagation through granite, from an explosive charge towards a shotcreted rock surface, has been studied. A type of finite element models suitable for dynamic analysis of shotcrete exposed to vibrations from blasting was developed and implemented using finite element software. It was demonstrated that wave propagation through rock towards shotcrete can be modelled using two-dimensional elastic finite elements in a dynamic analysis. It will be possible to describe the propagation of the waves through the rock mass, from the centre of the explosion to the reflection at the shotcrete-rock interface. Examples of preliminary recommendations for practical use are given in (Ahmed 2015), and it is demonstrated how the developed models and suggested analytical technique can be used to obtain further detailed limit values.

In underground opening excavation, the millisecond (ms) delay blasting technique is used to reduce the charge weight in a single fire for meeting the safety control criterion (Yang et al. 2016). In this study, cases with multiple explosive charges are studied, aiming at finding the effects of the vibrations induced with delay times. The models are here also further developed

by considering the loading plan for the blasting rounds by assuming initiation of explosives with a time interval within the rock mass,.

1.2 Rock support with shotcrete

The main design principle for rock support in underground construction is to help the rock carry its inherent loads. There are many elements, which are used in rock support systems; e.g., shotcrete, rock bolts, steel arches, mass concrete or prefabricated elements, used solely or in combination. In Sweden, shotcrete is widely used in rock support due to the quality of the rock, i.e. hard rock. Shotcrete is sprayed on the rock surface after the excavation of tunnel or a rock cavern to prevent fallout of rock blocks, thereby securing the arch-shape of the tunnel profile. The most fundamental characteristic of shotcrete is its ability to adhere to a surface, forming a bond that depends on the bond strength between shotcrete and rock. The first type of shotcrete support consists of only a single un-reinforced shotcrete lining that bonds to the rock surface. Other types are shotcrete linings anchored in fully grouted rock bolts or end-anchored rock bolts. For these, the shotcrete lining must be reinforced with steel mesh or fibres. Another type is shotcrete arches, built up by plain or fibre-reinforced shotcrete.

Rock support is usually designed for static loading conditions, but in some cases, the openings are also subjected to dynamic loads. One example is the detonation of explosives during excavations of tunnels and underground spaces. These detonations lead to stress waves that propagate through the rock and may cause severe damage to installations and support such as shotcrete.

There are few studies that measured the bond strength (Saiang et al. 2005, Bryne 2014) and most of these have been performed under static loads. Only two studies (Ahmed 2012a, Ansell 1999) measured the bond strength while exposing shotcrete to impact-type vibration during the setting period. Some bond test methods have been developed to estimate the bond strength between shotcrete and rock. There are for example non-destructive evaluation methods based on the impact-echo method that can be used to detect partial de-bonding or voids between shotcrete and rock, see e.g. Song and Cho (2009 and 2010). To obtain a measure of the bond strength destructive tests such as pull-out tests must be performed. Holmgren (1987) studied the modes of shotcrete failure using punching block tests to simulate loads applied on a shotcrete lining. The test results indicate that for steel fibre and mesh reinforcement linings, direct shear failure tends to occur when the bond to the rock mass is good, while flexural and punching shear failure occur when the bond is poor, causing debonding. Other possible modes of shotcrete failure include bending, compressive and tensile failures, but these are not relevant for the cases studied here.

Hahn and Holmgren (1979) suggested that the bond strength should be set to 0.5–1.0 MPa at 28 days. However, in cases where significant fractures or other planes of weakness exist parallel to the shotcrete rock interface, it must always be assumed that the effective bond strength will be low (Barrett and McCreath, 1995). Low bond strength will also occur for surfaces not initially cleaned, which means that the bond strength can be improved by first washing the rock surface using high-pressure water. Malmgren and Nordlund (2008) investigated the influence of surface treatment of rock (water jet scaling), shrinkage and hardening of shotcrete on the bond strength. It was concluded that the bond strength, in that case, was 0.33 MPa and 0.68 MPa for normal treatment and water-jet scaling, respectively. Saiang et al. (2005) performed a series of laboratory tests on cemented shotcrete-rock joints, to investigate the strength and stiffness of the interfaces. The load at which two jointed pieces came apart was considered as the bond strength. The average bond strength of 0.56 MPa was obtained. A series of tests with a new approach for testing the bond strength between young shotcrete and a concrete plate was performed by Bryne et al. (2011). The tests indicated a relatively rapid development of the bond strength which reached 1.0 MPa after 24 hours. This is in good correspondence with the range of 0.6–1.1 MPa reported from other investigations on 1–2 days old shotcrete and mortar. The above bond strength values obtained for young, and hardened shotcrete are summarised in Table 1.1. The data presented in Table 1.1 gives a comparison between values for varying rock quality and test methods. Due to the difference in size of the test samples and the varying quality of the rock and concrete, the data presented in different papers treating the bond strength of bonded and unbonded contacts is rather problematical.

Table 1.1: Bond strength at the shotcrete-rock interface obtained from tests (Ahmed 2012b).
Vidhäftningshållfasthet i gränssnittet mellan sprutbetong-berg. Erhållen vid vidhäftningsprov (Ahmed 2012b).

	Bond strength	Comments
Hahn and Holmgren (1979)	0.3 – 1.7 MPa	Granite
Malmgren and Nordlund (2008)	0.33 MPa 0.68 MPa	Normal treatment Water-jet scaling
Saiang et al. (2005)	0.56 MPa	Shotcrete-rock joints
Bryne et al. (2011)*	0.06 – 0.07 MPa 0.36 MPa 0.35 – 0.48 MPa 0.67 – 0.83 MPa 0.74 – 1.15 MPa	Age: 6 hours 10 hours 12 hours 18 hours 24 hours

*Bond strength between shotcrete and concrete.

1.3 Previous research

The performance of young and hardened shotcrete exposed to high magnitudes of vibration is investigated in Ahmed and Ansell (2012a, 2012b and 2014) and Ahmed et al. (2012). Safe distances and shotcrete ages for underground and tunnelling construction are discussed, using numerical analyses and comparison with measurements and observations summarised in (Ansell 1999). Examples of preliminary recommendations for practical use are given in (Ahmed 2015), and it is demonstrated how the developed models and suggested analytical technique can be used to obtain further detailed values.

As a first step towards reliable guidelines for how close, in time and distance, to young and hardening shotcrete blasting can be allowed, in-situ tests were conducted by (Ansell 1999) in the Swedish mine at Kiirunavaara. The observed vibration levels showed that sections of shotcrete had withstood high particle velocity vibrations without being seriously damaged. It was concluded that shotcrete without reinforcement, also as young as a couple of hours, can withstand vibration levels as high as 500−1000 mm/s, while section with loss of bond and ejected rock where found for vibration velocities higher than 1000 mm/s. Similar measurements, based on in-situ experiments conducted in Japan (Nakano, 1993), showed that vibration velocities of 700 mm/s cracked the observed shotcrete lining. The response of steel fibre-reinforced and steel mesh reinforced shotcrete linings subjected to blasts was investigated in a Canadian mine (McCreath et al., 1994). It was observed that the shotcrete remained attached to the rock surface for vibration levels up to 1500–2000 mm/s, with only partial cracking observed in the shotcrete. Maximum vibration levels are often defined regarding peak particle velocity (PPV). Table 1.2 shows that bond between shotcrete and rock can withstand PPV levels of range 500–2000 mm/s before bond damage occurs.

Table 1.2: Vibration velocities PPV when bond damage occurs. Based on in-situ measurements.
Vibrationshastigheter PPV, då bortfall av vidhäftning mellan berg och sprutbetong sker. Baserat på fältmätningar.

	PPV	Comments
Kiirunavaara, Sweden (Ansell 1999)	500−1000 mm/s	Young shotcrete
Tunnelling, Japan (Nakano, 1993)	up to 700 mm/s	
Gold mine, Canada (McCreath et al., 1994)	1500–2000 mm/s	Steel fibre-reinforced and steel mesh-reinforced shotcrete

The recommendation of minimum ages of shotcrete at the time of blasting, exemplified with the recommendations for 100 mm thick shotcrete is presented by Ahmed (2012b) and Ahmed and Ansell (2014) and is here presented in Table 1.3. Three different shotcrete types are

included in Table 1.3. The results from Ansell (2007) are given for comparison as representative for slow hardening shotcrete with water glass (Sodium silicate) and low-temperature curing. The results in Table 1.3 are calculated for detonations of 0.5, 1.0, 2.0 and 3.0 kg of explosives at 2.2, 3.0 and 5.0 m from shotcrete on a granite rock surface.

Table 1.3: Recommended minimum ages in hours for 100 mm thick shotcrete of three types (Ahmed 2015).
Rekommenderad minimiålder i timmar för 100 mm tjock sprutbetong av tre typer (Ahmed 2015).

	Distance from explosive									
	2.2 m			3.0 m				5.0 m		
Explosives:	0.5kg	1.0kg	2.0kg	0.5kg	1.0kg	2.0kg	3.0kg	0.5kg	1.0kg	2.0kg
Ahmed (2012b)	12	18	*	10	13	21	-	7	9	12
Ansell (2007)	>24	>48	*	24	>24	>48	-	9	21	>24
Ahmed and Ansell (2014)	-	-	-	-	12	15	23	-	-	-

* Not possible to obtain a sufficiently high bond strength. - Data not calculated.

1.4 Aims

In this study, numerical modelling was performed to exam the behaviour of shotcrete linings on moderately jointed hard rock under blasting loads. A dynamic analysis method that realistically captures the characteristics of the blasting load was developed. The main goal was to recommend a finite element based analysis model, describing how the blasting load can be practically applied and how the resulting stress wave propagation can be modelled and described numerically.

One further objective of this study is to assess how the suggested type of analysis models can be used for the case with shotcrete on fractured rock walls subjected to blasting with delay time. One important question here is how the behaviour of shotcrete differs, for example with respect to failure types. The goal is here to investigate how a criterion for multiple explosive charges should be formulated.

Chapter 2

Previous in situ investigations

This section describes in situ tests performed to characterise the vibrations that occur along tunnel walls during excavation blasting. The tests, thoroughly described by Ansell (1999), Reidarman and Nyberg (2000) and Nyberg et al. (2008) give data for the investigation and demonstration of how measurements are conducted. The measurements used for comparison and verification of the numerical results presented in the flowing chapters are summarised.

2.1 Monitoring of vibrations during blasting

Some attempts have been made to investigate the effect on shotcrete from blasting. In-situ tests, conducted underground in the Swedish mine at Kiirunavaara (Ansell 1999), was a first step towards the understanding of the vibration resistance of young shotcrete. The tests were conducted with sections of plain, un-reinforced shotcrete projected on tunnel walls and exposed to vibrations from explosive charges detonated inside the rock at ages of 1 to 25 hours, as shown in Figure 2.1. During these three measurement projects accelerometers were placed on a horizontal line along the length of the tunnel, two accelerometers at each measurement point to provide a two-axial description of the vibrations, parallel with and perpendicular to the length of the tunnel. Surface mounted accelerometers were placed on steel or aluminium plates bolted to the rock. For measurements inside the rock, accelerometers were mounted inside fully grouted pipes of PVC. The inner end of these pipes consisted of a conical tip, of steel or aluminium that was in contact with the rock and contained holders for the accelerometers on the inside. The lengths of the pipes were in these cases adjusted so that the measurement points were positioned about 300 to 500 mm behind the rock surface. The obtained acceleration measurements provided a good set of data for the evaluation of the analytical and numerical models with respect to the risk for local shotcrete damage in the vicinity of the source of blasting. It was concluded that shotcrete without reinforcement, also as young as a couple of hours, can withstand vibration levels as high as 500−1000 mm/s while section with the loss of bond and ejected rock were found for vibration velocities higher than 1000 mm/s. The results

also provided information about stress wave propagation in hard rock, and a scaling relation for PPV as a function of distance and explosive charge weight.

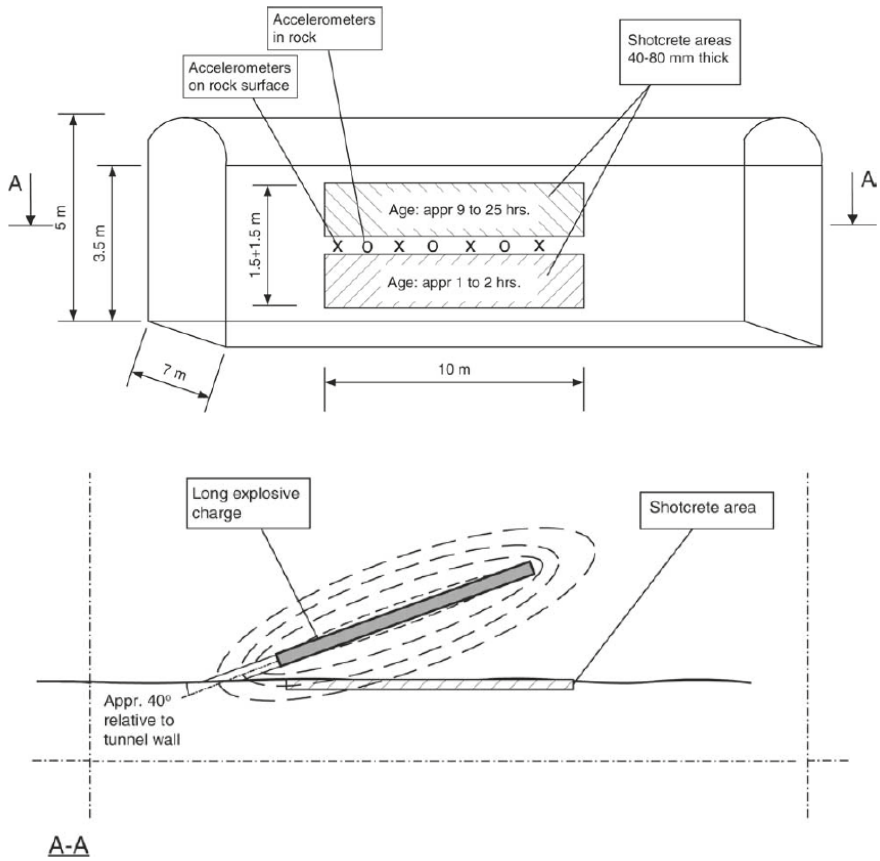

Figure 2.1: Schematic view of the test site. Explosive charge in the rock behind shotcrete areas, from (Ansell 1999).
Skiss av provplatsen. Sprängladdning i berg bakom betongsprutade områden, från (Ansell 1999).

However, an attempt to characterise the vibrations that occur along tunnel walls during excavation blasting has been performed by Reidarman and Nyberg (2000). The investigation was performed during construction of the Southern Link (Södra länken) road tunnel system in Stockholm, Sweden, and comprised visual inspection of the shotcrete lining to detect cracks and damages. The accelerometers used were positioned following the same system as for the Kiirunavaara measurements, described above. No shotcrete damage was observed following the blasting, due to the very strict guidelines used, and it can thus be assumed that the shotcrete-

rock system behaved elastically throughout the passage of the stress waves. The measurement of vibrations from four blasting rounds was performed using accelerometers located along an axis stretching approximately 5-50 meters behind the tunnel front. Accelerations were measured in two directions, parallel with and perpendicular to the tunnel walls, recorded and later numerically recalculated into corresponding velocity-time records. All measurement points were situated 300 mm into the rock. The layout of the test tunnel with the position for the measurement points is shown in Figure 2.1. It should be noted that the advancement of the tunnel front is towards the left in the figure and that each blasting round results in 5 m of new tunnel length, except for the third round which gave a 10 m extension. The figure also shows how some measurement points were abandoned in favour of new points closer to the tunnel face, thus approximately giving equal spacing between the points for each of the four rounds.

The maximum velocities for each measurement point versus the distances along the tunnel wall are shown in Figure 2.3, where it can be seen that the largest PPV levels were recorded within the nearest 20-30 m to the explosives.

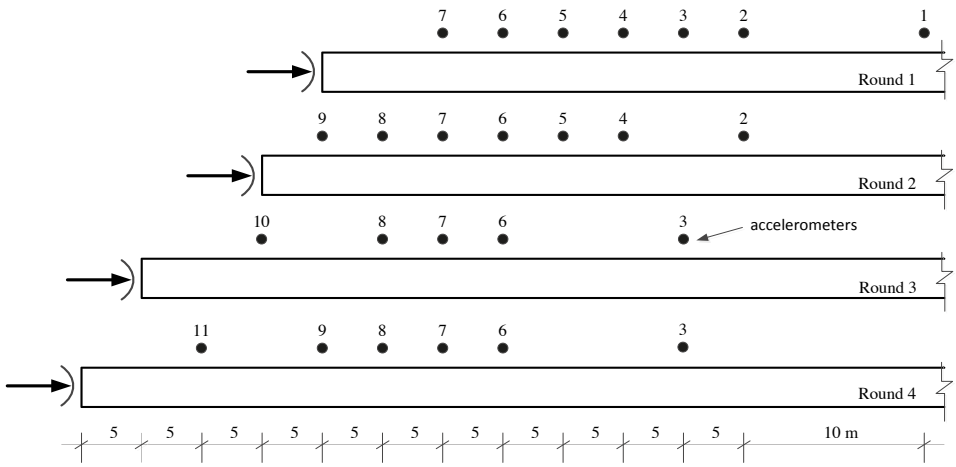

Figure 2.2: Tunnel with advancing front during four excavations rounds. Test layout with positions of measurement points, from Ahmed and Ansell (2016).
Tunnel med propageranda front under fyra utgrävningssteg. Försöksplan med positioner för mätpunkter, från Ahmed and Ansell (2016).

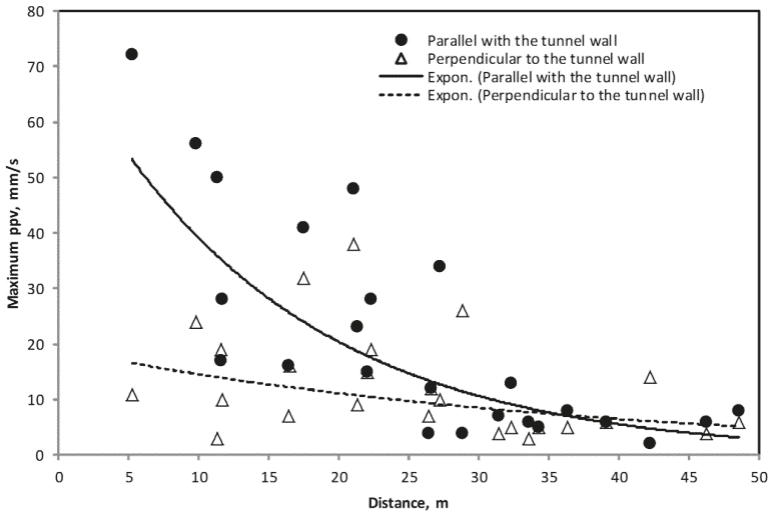

Figure 2.3: Maximum PPV versus distance along the tunnel wall, from Ahmed and Ansell (2016).
Maximal PPV för varierande avstånd längs tunnelns vägg, från Ahmed and Ansell (2016).

As an attempt was made to study the pillar stability between vertical canister full-face holes, a 70 m long tunnel named APSE (Äspö Pillar Stability Experiment) was blasted in hard crystalline rock at the Äspö HRL (Hard Rock Laboratory) in Sweden (Nyberg et al. 2008), see Figure 2.4. The APSE tunnel was blasted in 34 top heading rounds and 12 bench rounds from the elevator shaft at level – 450 m. The vibration measurements consist of three data sets. The first set of data consists of vertical geophone data for blast optimisation and vibration control approximately 10–600 m away from the 46 rounds. The second data set consists of accelerometers grouted into gauge holes along the tunnel wall 14–28 m behind the front. This set was primarily used for a function control of the contour blast holes of the three last rounds, but the measurements were also used for calculation of the P-wave velocity and the amplitude attenuation along the tunnel wall. The third data set consists of measurements 600–1600 m from the blasts for calculation of the far-field amplitude attenuation. Seismograph stations on the ground surface were used for collection of these data. The results show that the PPV did not exceed the upper limit 50 mm/s for installations and facilities and that moderate disturbances very unlikely will occur above ground 450 m away from the tunnel. Over a range of 350 m distance, the mean PPV decreases about 100 times.

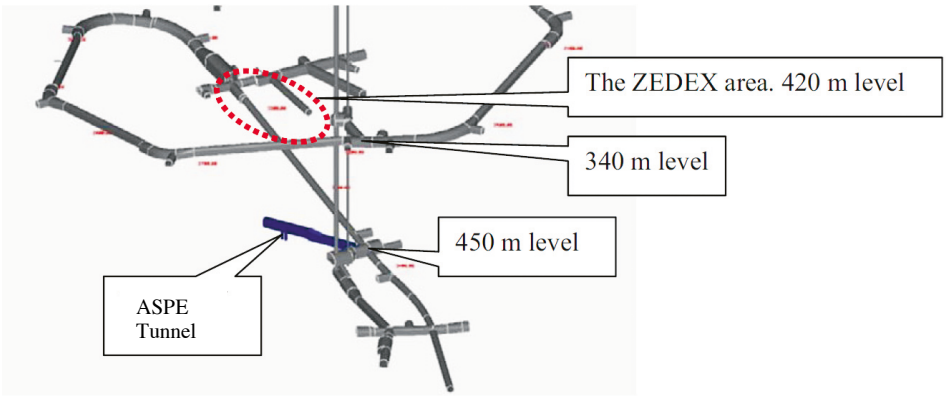

Figure 2.4: Layout of the ASPE Tunnel (Nyberg et al. 2008).
Skiss av ASPE Tunneln (Nyberg et al. 2008).

The geophones were used to register the vibrations generated by 46 blast rounds at distances of 10–600 m. Figure 2.5 shows the geophone positions below the 340 m level (the geophones PD0016B01) that were used for vibration underground level control on installations and constructions (Nyberg et al. 2008). All geophones (channels) were set with a rather low trigger level (0.2 mm/s) to guarantee that no data were missing. The acquired PPV data represents wave propagation caused by blasting at a remote point, e.g. at the tunnel front. The most important types of stress waves in rock are longitudinal waves (P-waves) and shear waves (S-waves), see Dowding (1996). Of these two types, S-waves are acquired because of the geophone mounting perpendicularly on the tunnel surface.

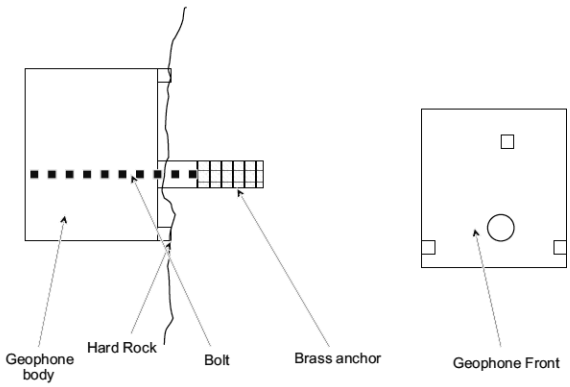

Figure 2.5: Layout of the geophone mounting (Nyberg et al. 2008).
Skiss av geofon monteringen (Nyberg et al. 2008).

The acquired PPV data of all rounds versus the distance is shown in Figure 2.6, where all recording units are included, for example the PPV-values from the integrated acceleration recordings and the seismographs. In Figure 2.6, it is clear that the PPV from the integrated acceleration recordings is higher than the standard geophone PPV at the same distances. This is probably due to the 350 Hz high cut filter that is used for the geophone recordings. The seismograph PPV is roughly within the distances of range 600–1600 m.

The results of this investigation are well suited for evaluation of the FE models described in Chapter 3. Therefore, the FE model can be used for a numerical study of the stress wave propagation from detonation through the rock towards the interface between the shotcrete and rock surface.

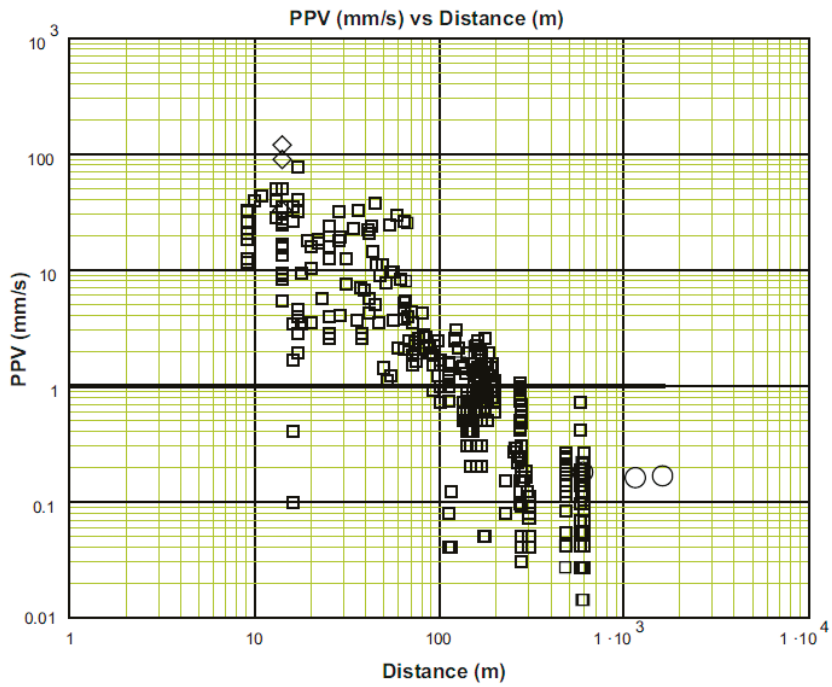

Figure 2.6: Maximum PPV for each round versus the distance. Symbols: □ Geophone 1 D data, ○ Seismograph 3D data and ◊ Accelerometer 1D data (Nyberg et al. 2008).
Maximal PPV för varje salva vid varierande avstånden. Symboler: □ Geofon 1 D data, ○ Seismograf 3D data och ◊ Accelerometer 1 D data (Nyberg et al. 2008).

2.2 Maximum PPV measurements

As shown in Figure 2.4, the particle velocities that can be measured remote from detonating explosives in rock will show a decrease in magnitude with increasing distance to the source of the explosion. This decay is caused by geometrical spreading and hysteretic damping in the rock (Dowding 1996). The maximum PPV of round 5-34 are compiled in Table 2.1, for a different amount of explosives and distances. The maximum measured vibration level is 49 mm/s. Based on maximum PPV in Table 2.1, the PPV as a function of the amount of explosives charged, at distances of 9 –19 m from the detonation, are presented in Figure 2.7. From Figure 2.7, it can be seen that the vibration amplitudes are increased corresponding to the amount of explosive at the distance of 9 m.

Table 2.1: Maximum PPV of rounds 5-34 at a distance of 9-65 m from the detonation. *Maximal PPV för salvor 5-34 vid avstånden 9-65 m från detonationen.*

Round	Distance (m)	PPV (mm/s)	Q (kg)
5	9	12.1	1.31
6	9	11.4	0.82
7	9	18.3	1.19
8	9	31.7	2.11
9	9	25.6	2.57
10	9	30.8	2.80
11	9	20.1	2.05
12	10	38.3	2.94
13	10	38.8	2.94
14	11	43.7	2.80
15	13	38.9	3.30
16	13	27.7	3.30
17	13	49.1	2.90
18	16	34.2	2.90
19	19	17.4	1.29
20	22	18.0	2.94
21	25	15.9	3.30
22	25	12.3	4.00
23	29	18.7	3.70
24	34	22.2	3.70
25	37	6.8	1.84
26	39	6.8	1.84
27	41	5.6	1.84
28	41	20.4	1.84
29	43	14	1.84

30	47	8.7	1.84
31	51	7.6	3.63
32	56	9.4	4.10
33	61	8.3	4.34
34	65	7.9	4.34

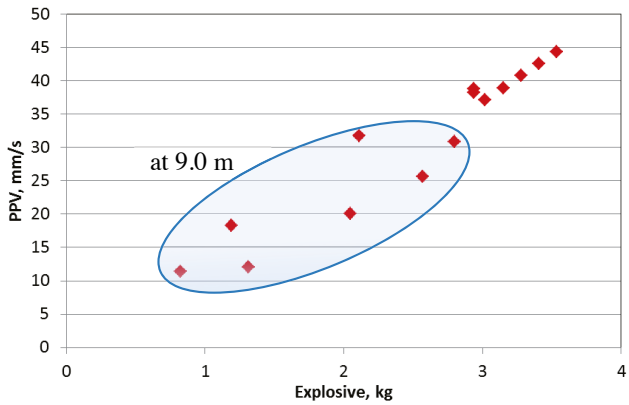

Figure 2.7: The maximum PPV of round 5 – 19 versus the amount of explosives at a distance of 9 – 19 m from the detonation.
Maximal PPV för salvor 5-19 vid varierande mängd sprängämne för avstånden 9-19 m från detonationen.

Chapter 3

Finite element analysis

The FE method is a powerful tool for the study of structures subjected to dynamic forces. Two-dimensional (plane strain) dynamic FE models of rock subjected to blast loading are presented, with the models, load formulations, and boundary conditions described. The propagation of the waves in the rock was here investigated by introducing the explosive material as a detonating point, or two points with a delay time. In this chapter, the FE model that consists of only rock with infinite boundary conditions was analysed. The results are used for comparison and verification of the FE model.

3.1 Finite element models

The models are here implemented using the FE program Abaqus/Explicit solver. The geometries of the FE models are created using the Abaqus/CAE interface. The fundamentals of the model was shown in Figure 3.1. The blasting loads are introduced as explosive material in a certain number of elements. The rock is discretized with first-order 4-node plane strain elements of type "CPE4R", recommended for simulations of impact and blast loading using the Abaqus/Explicit (Abaqus 2014). Far-field conditions on the top, bottom and right-hand side boundaries are modelled using infinite elements of type "CINPE4". The element size of the shotcrete part is 0.012×0.012 m^2.

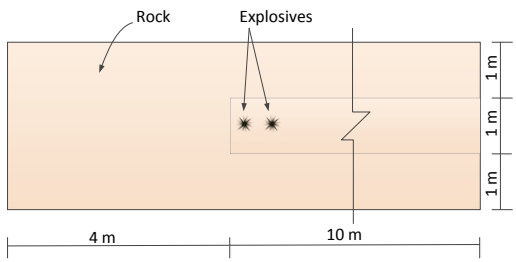

Figure 3.1: Configuration of the finite element model with only the rock.
Konfiguration av den finita elementmodellen, med endast berget.

3.2 Material properties

In this report, the examples have been performed based on the properties of the hard crystalline rock at the location of the Äspö HRL (Nyberg at el. 2008).

3.2.1 Rock

It is difficult to define material properties for a fractured rock mass since its behaviour is site-specific. Its properties depend on geological discontinuities, e.g. fractures or zones containing weaker materials, that are the results of historical geological events. However, the mechanical properties of the 450 m level of the Äspö HRL are presented by Andersson (2003), given in Table 3.1. Since the Mohr-Coulomb plasticity model can be used for design applications in the geotechnical engineering area, the Abaqus Mohr-Coulomb model was used in this study, for more details see (Abaqus 2014).

Table 3.1: Mechanical properties of the rock mass.
Mekaniska egenskaper för bergmassan.

Young's modulus	55 GPa
Poisson's ratio	0.26
Friction angle	41 Degrees
Cohesion	16.4 MPa
Tensile strength	14.3 MPa

3.2.2 Detonation

The Abaqus (Abaqus 2014) software is one of the few codes that allow an accurate description of explosive detonation and explosive-rock interaction. In Abaqus, the explosion is implemented by an equation of state (EOS). The Jones-Wilkins-Lee (JWL) EOS describes the relationship between volume, energy and pressure of detonation products and is widely used in the simulation of blasts. The JWL EOS is defined as:

$$p = A\left(1 - \frac{\omega\rho}{R_1\rho_0}\right)\exp(-R_1\,\frac{\rho_0}{\rho}) + B\left(1 - \frac{\omega\rho}{R_2\rho_0}\right)\exp(-R_2\,\frac{\rho_0}{\rho}) + \omega\rho E_m \qquad (1)$$

where p is the detonation pressure, ρ_0 is the relative volume, E_m is the internal energy per initial volume, and A, B, R_1, R_2, and ω are parameters related to charging explosives. In the numerical

simulation, the explosive density is assumed to be 1300 kg/m^3 and the velocity of detonation is 4000 m/s. The parameters associated with the JWL equation should be obtained by experiments, but direct measurements of these parameters were not carried out here. Instead, these parameters in the simulation are given A = 214.4 GPa, B = 0.182 GPa, R_1 = 4.2, R_2 = 0.9, ω = 0.15, and E_m = 4.192 GPa by referring to the work of Yang at el. (2016), in which the explosive is also used and the simulated results of rock where the mechanical properties agree well with those obtained by site investigations (Section 3.2.1).

3.2.3 Shotcrete

This study assumes un-reinforced shotcrete, without fibre content and with a standard composition containing water glass as an accelerator. The material properties chosen for the examples resembled that of the shotcrete used in the Kiirunavaara tests (Ansell 2004) resulting in a density of 2100 kg/m^3 and a modulus of elasticity of 27 GPa after 28 days. However, there is no need to include non-linear effects in the present model since the load here does not exceed the tensile strength of the shotcrete.

3.3 Model verifications

The propagation of the waves in rock without shotcrete was investigated with the purpose to demonstrate the choice of material properties. A verification of the suggested FE model was done by comparing numerical results with corresponding measurements. As previously described the acquired measurements from the APSE tunnel (Nyberg et al. 2008) were chosen for the comparison and the parameters in the material constitutive models, therefore, correspond to Table 2.1, wherever possible. The explosion was implemented by EOS (as described in Section 3.2.2).

The finite element model here consists of rock and infinite boundary conditions without shotcrete, see Figure 3.2. A series of examples have been analysed using a various amount of explosives 1.1 and 2.8 kg, represented in 6 and 15 square shaped elements with a side length of 0.012 m, respectively, as shown in Figure 3.2.

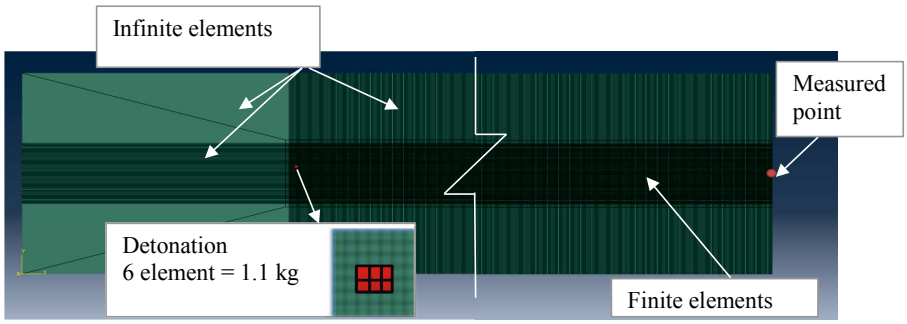

Figure 3.2: Finite element model.
Finit elementmodell.

The velocity – time histories calculated in the directions parallel with and normal to the tunnel wall are presented in Figure 3.3 (a) and Figure 3.3 (b), respectively. Based on the obtained results in Figure 3.3 (a), the simulated maximum PPVs of 20.6 and 35.8 mm/s corresponding to the amount of explosive 1.1 and 2.8 kg, respectively, are given in Table 3.2. The results from Table 2.1 are also given in Table 3.2 for verification. As seen, the obtained PPV of 20.6 mm/s with 1.1 kg explosive is close to the measured value 12.1, 11.4 and 18.3 mm/s at 9 m from detonation. Correspondingly, the simulated result of 2.8 kg explosive gives PPV of 35.8 mm/s that is in good agreement with measured PPV of 31.0 and 38.0 mm/s at a distance of 9 and 10 m from the detonation with 2.8 and 2.9 kg explosives, respectively. The velocity-time histories obtained in the direction normal to rock surface are also shown in Figure 3.3 (b). The maximum PPVs that occur at the rock surface are 540 and 980 mm/s for 1.1 and 2.8 kg explosives, respectively.

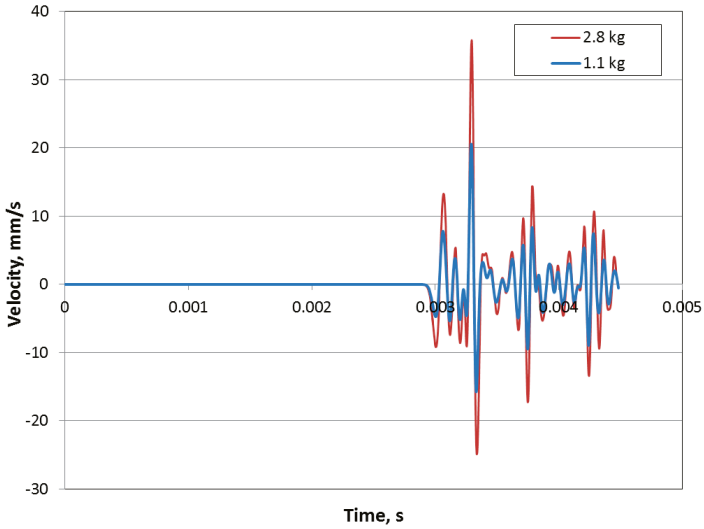

(a)

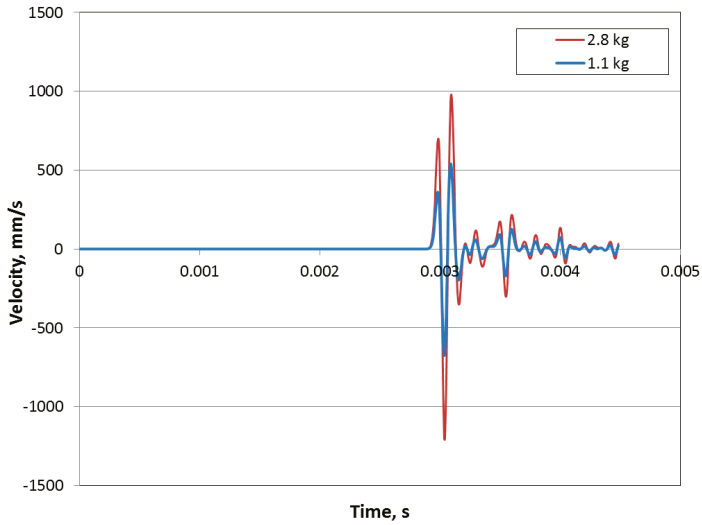

(b)

Figure 3.3: Calculated velocity – time histories for various amount of explosive at the free surface of rock (a) parallel with the rock surface, and (b) normal to rock surface. The distance from the detonation equals to 9.5 m.
Beräknad hastighet – tid för olika mängd sprängämne vid den fria bergytan (a) parallellt med bergytan, och (b) normalt mot bergytan. Avståndet från detonationen är 9,5 m.

Table 3.2: Simulated and measured PPV.
Simulerad och uppmätt PPV.

	PPV mm/s	Amount of explosive, kg	Comments
FE Models	35.8	2.8	The distance from the detonation equals to 9.5 m
	20.6	1.1	
Measurements (Nyberg et al. 2008)	31.0	2.8	At 9.0 m from detonation
	38.0	2.9	At 10.0 m from detonation
	12.1	1.31	At 9.0 m from detonation
	11.4	0.82	
	18.3	1.19	

Chapter 4

Results and discussions

Numerical results from different models are presented. In this chapter, the FE models are used to simulate the stress waves from blasting, propagating in rock towards shotcrete on a tunnel wall, with shotcrete bonded to intact and jointed rock.

4.1 Shotcrete bonded to rock

The interaction between rock and shotcrete was modelled using tie constraints, i.e. no relative displacement between the materials was assumed. The model demonstrates the waves propagating through the rock from the detonation point, towards the bonded shotcrete at the tunnel side. The dimensions of the models are shown in Figure 4.1. Plane strain elements were used implementing a non-linear rock material model, capable of describing cracking during the detonation. Results for 100 mm thick shotcrete were studied. The explosive charges were here located at 9.5 and/or 9.0 m from the shotcrete-rock interface. In this model, the stress waves reached the shotcrete in an oblique angle, and a domination of shear stresses is also observed.

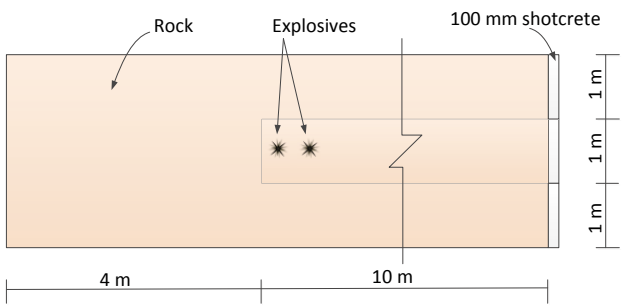

Figure 4.1: Configuration of the finite element model.
Konfiguration av finita-elementmodellen.

The models describe three cases with respect to the position of the explosive points (P1) and (P2), see Figure 4.2. The first case was used for studying the effects of stress wave propagation along the tunnel side; from an explosive charge at one point (P1) mounted at 9.5 m from the shotcrete-rock interface, as shown in Figure 4.2 (a). The models consider the loading plan for the blasting rounds, i.e. initiation of explosives with a time interval. Thus, in the second case, two points of explosive charges (P1) and (P2), with a delay time of 1 ms, were studied. The two explosive points were mounted at the same level, at 9.5 and 9.0 m from the shotcrete-rock interface, respectively, see Figure 4.2 (b). The third case is that the two points of explosive were both mounted at 9.5 m from the shotcrete-rock interface, also with a delay time of 1 ms, as shown in Figure 4.2 (c).

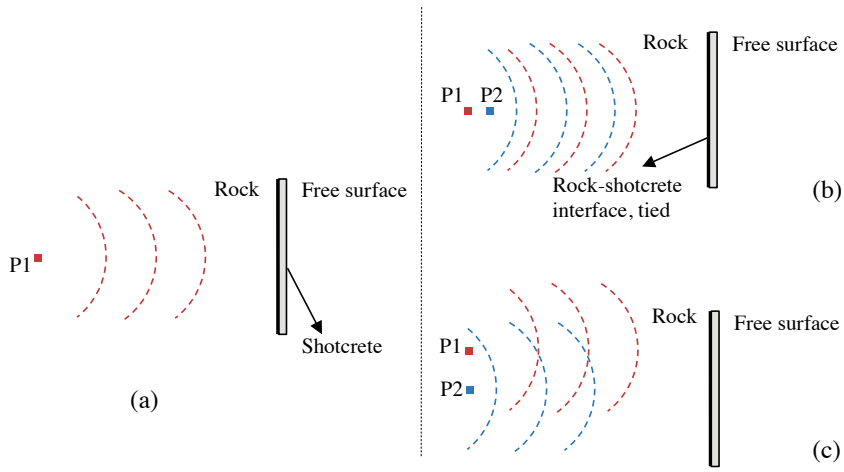

Figure 4.2: Examples of explosive positions in, (a) explosive charge of 2.8 kg at distance 9.5 m from the shotcrete-rock interface, (b) explosive charges of 2.8 kg at distances 9.5 m and 9 m from the shotcrete-rock interface, and (c) explosive charges of 2.8 kg at distance 9.5 m that located vertically.
Exempel på laddningsplaceringar för (a) sprängladdning 2,8 kg vid avståndet 9,5 m från gränsskiktet mellan berg och sprutbetong (b) sprängladdningen 2,8 kg vid avstånd 9,5m och 9,0 m från gränsskiktet mellan berg och sprutbetong, och (c) sprängladdningen 2,8 kg vid avstånd 9,5 m som ligger vertikalt.

A local view of the finite element model where the blasting was induced, two different positions of the explosive charge corresponding to case (b) in Figure 4.2, are simulated with the delay time of 1 ms, is presented in Figure 4.3. When explosive charges are detonated at first in (P1), intense dynamic stresses are initiated around the detonated point, which represented the instantaneous acceleration of rock masses caused by the energy of the detonation. The stress waves spread away from the source into the surrounding rock masses toward the free surfaces. After 1 ms, the second point (P2) was detonated and the stress waves complied with previous stress waves caused by the first detonation of (P1).

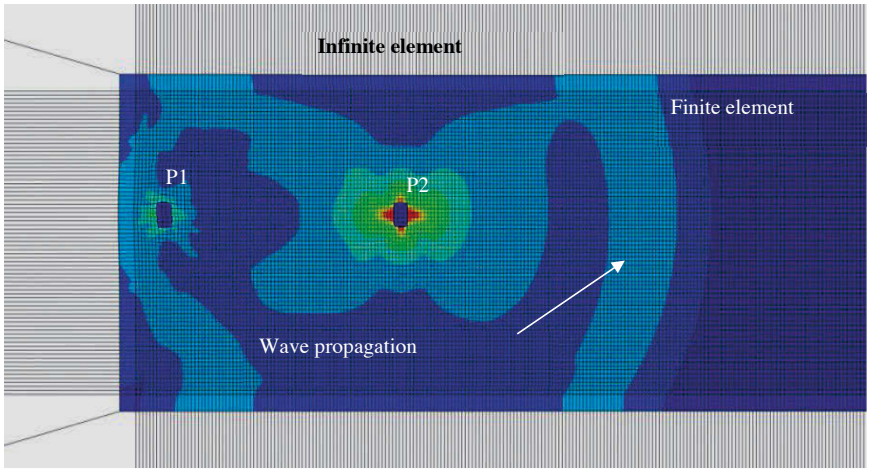

Figure 4.3: Local view of the finite element model used for numerical analysis of blasting vibration.
Lokal vy av finita elementmodellen som används för numerisk analys av sprängning vibrationer.

The response of the shotcrete in the tunnel from the three cases was investigated for induced blasts, using 2.8 kg of explosives in each explosive point. The response of 100 mm shotcrete for various explosive charges and positions are shown in Figure 4.4. This figure shows comparisons of the stress-time histories at the shotcrete elements closest to the rock surface, calculated for the three cases described in Figure 4.2. The stresses are indicated with the positive sign representing tensile stresses and the negative sign representing compressive stresses. The results in Figure 4.4 show that when the explosion was induced the compressive stress waves propagate towards the free faces, where they are reflected as tensile stress waves. The reflection waves are superimposed onto the initial compressive stress waves in the process of propagation, i.e. case (a) in Figure 4.2, and onto new compressive stress wave from the detonation at point (P2), i.e. case (b) and (c) in Figure 4.2. Thus, this will influence the tensile stress waves of shotcrete-rock interface.

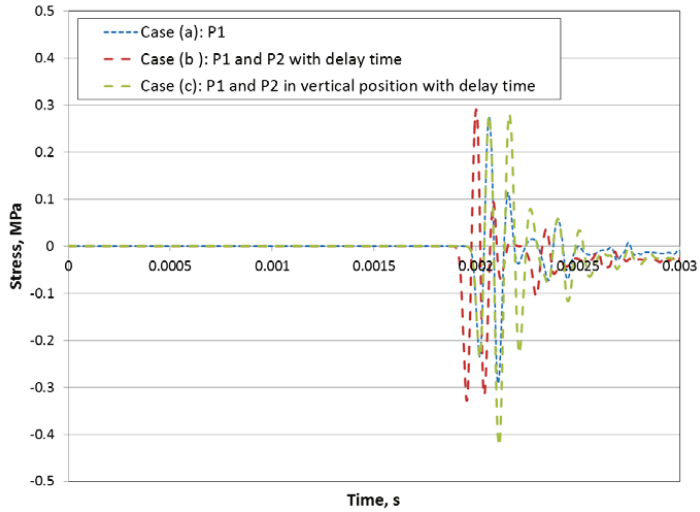

(a)

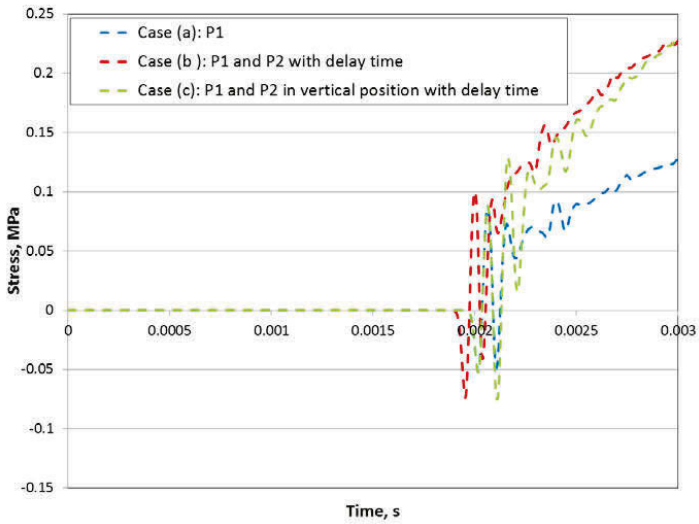

(b)

Figure 4.4: Comparison of the stress–time histories for three cases presented in Figure 4.1, (a) normal to and (b) parallel with the tunnel wall.
Jämförelse av tryck- tidförlopp för de tre fall som presenterades i Figur 4.1, (a) vinkelrätt och (b) parallellt med tunnelväggen.

It can be seen from Figure 4.4 (a) that the stress-time history in the direction normal to the tunnel wall of case (b) has an almost similar form as one of the single explosive points, i.e. case

(a), but with a higher peak and shorter rising time. The reduction in the rise time is probably caused by the superposition of blasting vibration of the two points (P1) and (P2) where the detonation of explosive point (P1) is accelerated by the vibrational energy of the detonation of explosive point (P2), and it follows that with the reduction of rise time a higher stress value is obtained. While in case (c), the stress-time history has two peaks with no reduction in rise time. It can also be seen that the stresses are 0.274, 0.291 and 0.274 MPa for case (a), (b) and (c), respectively. The rise time is short, i.e. it starts from 0.17 ms and ends around at 2.2 ms. This short rise time is caused by the superposition effect when the wave immediately reaches the interface and then, due to the thin layer of the shotcrete, directly reflects at the free surface and transmits back into the rock. During this period, the maximum stresses develop. After this period, the response shows a free vibration mode. It should be pointed out that the analysis covered 3 ms duration.

An example of the distribution of tensile stress in rock and shotcrete in the normal direction to the tunnel wall is shown in Figure 4.5. The stresses are indicated with red areas showing tensile stresses greater than 0.1 MPa while the grey is showing compressive stresses lower than zero. High tensile stress response of shotcrete can be seen forming close to the rock surface, giving stress concentrations along almost 0.5 m length. Such stresses also propagated through the rock, representing the reflected compressive stress waves as previously mentioned. The stresses in the direction parallel with the tunnel wall are also simulated and presented in Figure 4.4 (b). It can be seen that up to 2.2 ms the stresses have a similar behaviour to those in the direction normal to the tunnel wall, see Figure 4.4 (a), with a higher second peak for case (b). After a longer time, the maximum responses develop during the free vibration mode for all models. In the model, the stress wave propagates from the detonation points through non-linear media, causing permanent displacements in the entire model. Figure 4.6 shows the displacement at the end of the analysis i.e. at 3 ms at the free surface. In this figure it is clear that the final displacement is 0.07 mm, which due to the permanent displacements is caused by the free vibration. Most of these displacements are in the direction parallel with the tunnel wall, giving higher stresses. For the computational time issue, the elastic material formulations were used for shotcrete since the strains do not exceed the elastic material strength. In the tunnel construction process explosive charges of 1– 4 kg are often used per each blast hole. Thus, for the higher blast loading the tensile strength does not exceed the elastic limit for this distance of 9.0 m from the detonation. It is, in this case, of little interest to continue the analysis for higher blast loading until damage of the shotcrete occurs. However, the stresses in the direction parallel with the tunnel walls will only be considered during the rise time. Thus, the stresses are 0.086, 0.095 and 0.124 MPa for cases (a), (b) and (c), respectively.

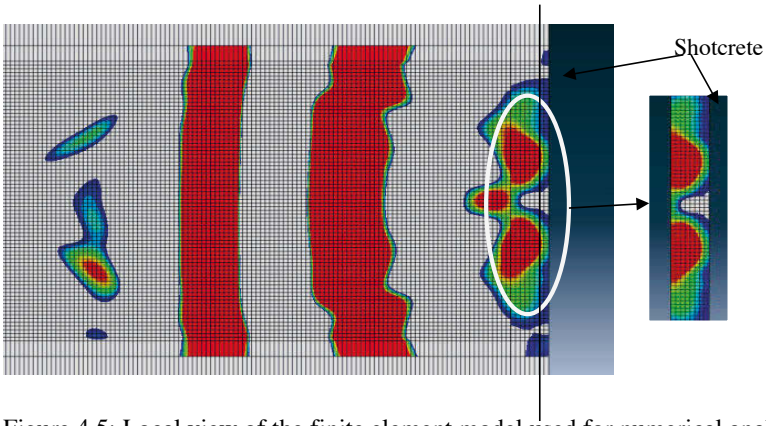

Figure 4.5: Local view of the finite element model used for numerical analysis of shotcrete.
Lokal vy av finita elementmodellen som användes för numerisk analys av sprutbetong.

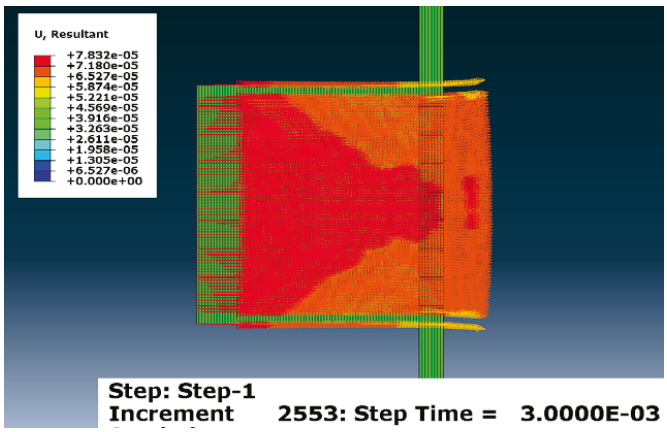

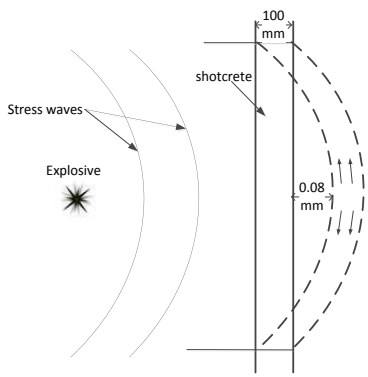

Figure 4.6: Displacement distribution of intact rock and shotcrete.
Förskjutning av intakt berg och sprutbetong.

4.2 Single rigid block

To increase the knowledge of the performance of shotcrete-rock interfaces exposed to vibration where poor rock condition exists; a modification of the geometry of the previous model is presented here. In the real case, during the excavation work, the rock area around the blast hole after the detonation contains cracks. Thus, planes of weakness exist parallel to the shotcrete-rock interface. A fractured rock zone of 0.5 m thickness along the tunnel walls are assumed. The fractured rock may be represented as a translating wedge, i.e. a single rigid body. The fundamentals of the models are shown in Figure 4.7. The detonation is introduced in three explosive points. The design of blocky rock was based on an experimental study performed by Holmgren (1975), with the height of the vertical sidewall of 0.5 m. The interaction between rock and shotcrete was modelled using tie constraints whereas the two surfaces of the intact rock, and blocky rock were modelled using the surface to surface interface with a coefficient of friction that is 0.6 (Ramana and Gogte, 1989), allowing separation between two surfaces. The element size of the shotcrete part is in the range of 0.012×0.012 m^2.

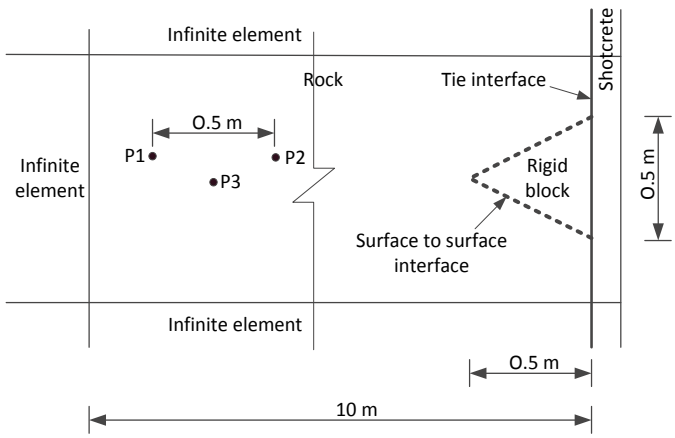

Figure 4.7: Configuration of the finite element model with a single rigid block.
Konfiguration av finita elementmodellen med ett styvt block.

The response of the shotcrete in the tunnel was also investigated for various blast load positions, using 2.8 kg of explosives in each explosive point. The vibrations induced by the detonation of three points are shown in Figure 4.8, for various time steps. It can be seen that after the detonation of point (P1), the stress waves caused by the detonation of the explosive point (P2) are superimposed onto the initial compressive stress wave, see Figure 4.8 (b). These stress waves were followed by that from the explosive point (P3), see Figure 4.8 (c). Under the blasting loads, the shotcrete stress along the lining length increased, giving stress concentrations around the blocky rock, see Figures 4.9 where the stresses in a direction normal to the tunnel

wall, are shown. The stresses are indicated with red areas showing tensile stresses (positive) over 0.1 MPa and blue showing compressive stresses (negative) lower than – 0.1 MPa. The area of the zero stress (green) can be assumed. It can be seen that at 1.8 ms after the detonation, the compressive stress waves reached the tip of the rock block, see Figure 4.9 (a), then travelled through the rock surrounding it towards the shotcrete-rock interface. The compressive stress waves reflected as tensile stress wave and the higher stresses are mainly concentrated at the corners between the rock block edges and shotcrete. Such stress concentrations also propagate parallel with the tunnel walls, but with decreasing stress levels. For these stresses, the stress-time histories of the shotcrete are presented in Figure 4.10. The results were calculated for two different numbers of explosives one and three explosive points, and compiled with the results of the previous model of intact rock, case (a) in Figure 4.2. In Figure 4.10 (a), it can be seen that the model with fractured rock gives lower stresses compared with the results when a model without fracture zone is considered. The stresses of the shotcrete normal to the tunnel walls are 0.291 and 0.093 MPa of intact rock (case (a)) and the model of blocky rock with one explosive point. Introducing the fractured rock in the model has a filtering effect on the propagation when vibration waves reach the shotcrete-rock interface. The waves are damped out when passing the blocky rock and thus there is no significant difference when the sequence of the explosives are introduced, e.g. for three explosive points, see Figure 4.10 (a).

The stresses in the direction parallel with the tunnel wall are shown in Figure 4.10 (b). It is to be noticed that similar trends of the stress-time histories are achieved, where the maximum responses develop during the free vibration mode. The stresses are also higher than in the case of intact rock due to that the blocky rock was allowed to separate during the analysis causing higher displacements as explained in Figure 4.11 (a). In this figure, the displacement at the end of the analysis, i.e. at 3 ms at the free surface, is 0.1 mm which is higher than the displacement of the intact rock and shotcrete case (Figure 4.6). In Figure 4.11 (b), the stresses are expected to converge towards the ultimate tensile stress. However, this behaviour needs to be verified through further numerical calculations.

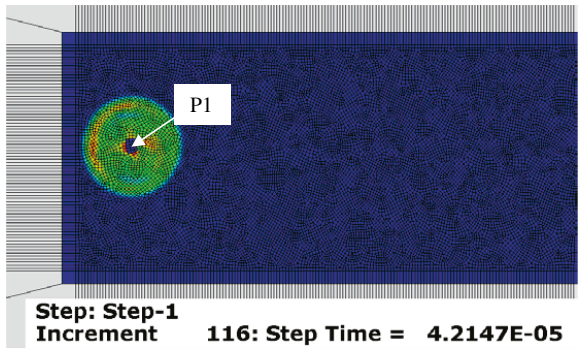

(a)

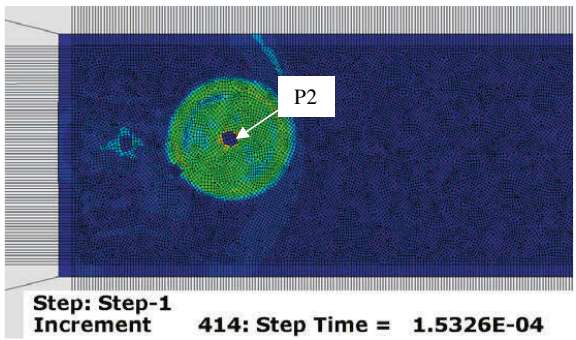

(b)

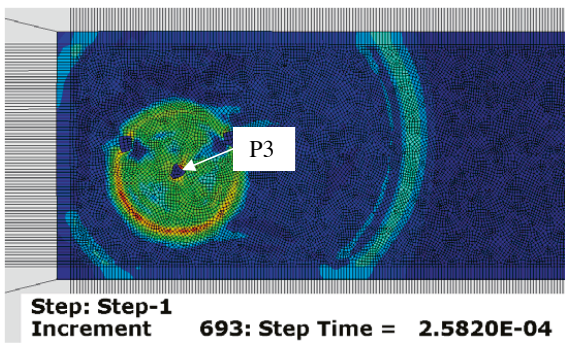

(c)

Figure 4.8: Local view of the finite element model with multiple blasting sources; detonation of the explosive points, (a) P1, (b) P2 and (c) P3.
Lokal vy av finit elementmodell med flera sprängämnesladdningars; detonation av laddningar i punkt, (a) P1, (b) P2 och (c) P3.

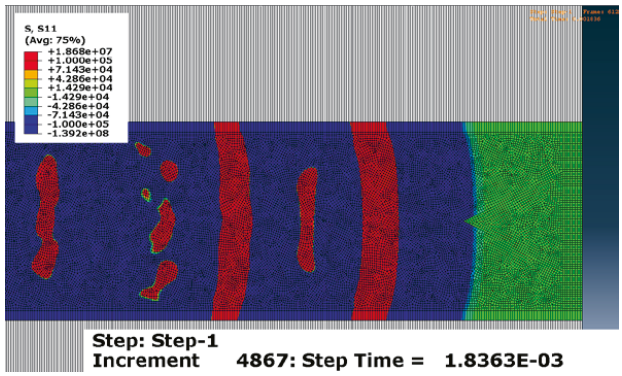

(a)

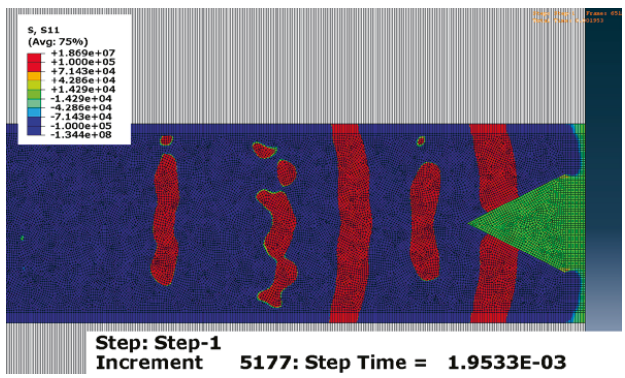

(b)

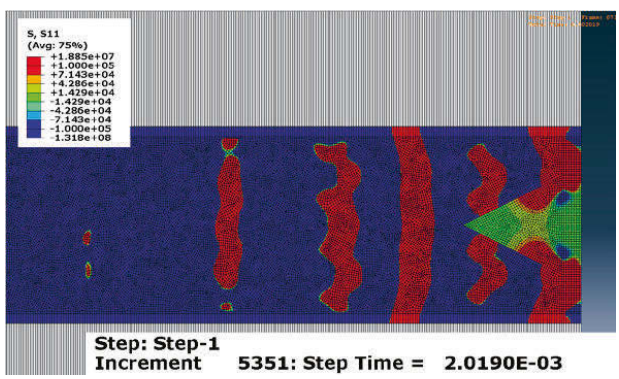

(c)

Figure 4.9: Local view of the finite element model with a rigid block at various time steps.
Lokal vy av finita elementmodellen med ett styvt block vid olika tidssteg.

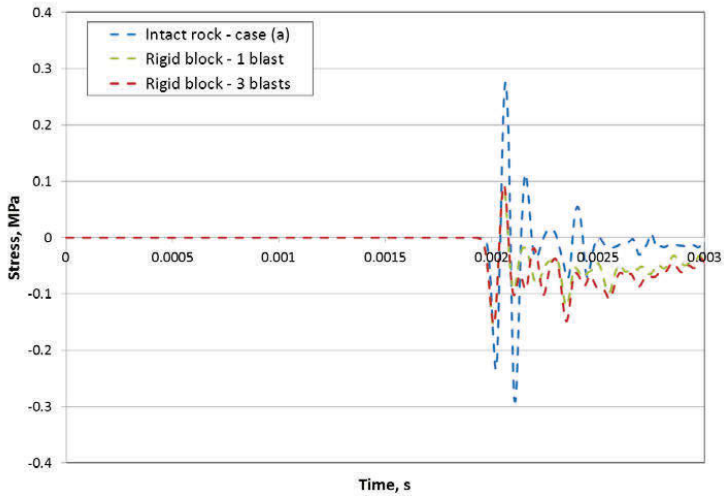

(a)

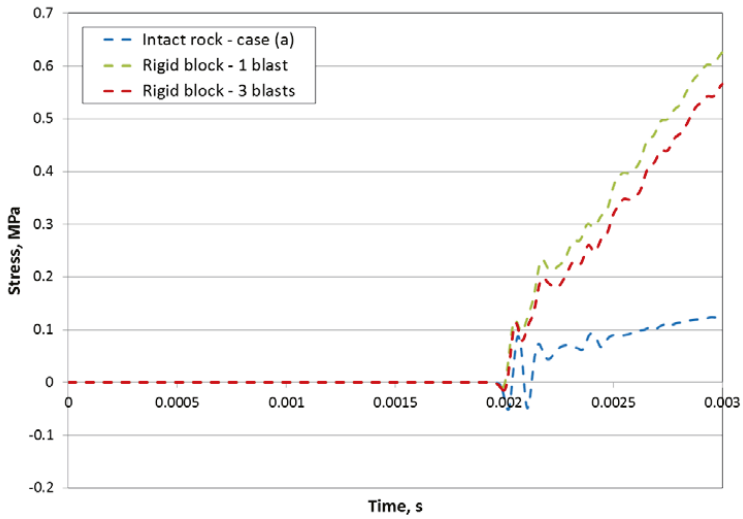

(b)

Figure 4.10: Comparison of the stress–time histories of shotcrete (a) normal to and (b) parallel with the tunnel wall.
Jämförelse av spännings-tidförlopp för sprutbetong (a) vinkelrätt och (b) parallellt med tunnelväggen.

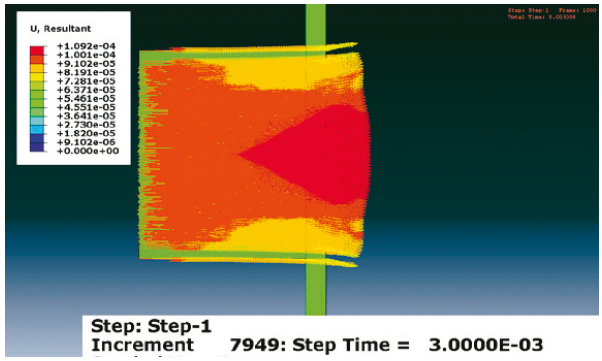

(a)

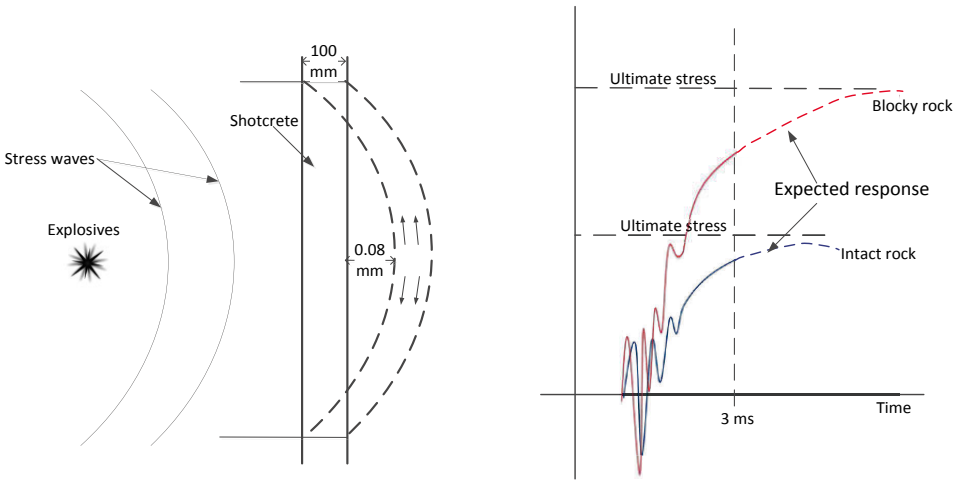

(b)

Figure 4.11: The single block model, (a) displacement distribution, (b) verified and expected response of the stresses.
Styvt block modellen, (a) förskjutning, (b) verifierad och förväntad respons av spänningarna.

Chapter 5

Conclusions

For the designers of mining and construction excavations, blast-induced vibrations are a major concern. Within this project, work on evaluating and proposing analytical models was made in several steps, with a focus on describing the behaviour of shotcrete on intact rock when the propagation of the waves in the rock is introduced as an explosive material within the FE model. At first, a comparison was made with measurements acquired during blasting for tunnel construction, see Section 2.2. The conclusion was that the plastic formulations of the rock were sufficient in this case and the application of blasting loads as an explosive material worked and gave realistic results.

It is also demonstrated and verified that wave propagation through rock towards shotcrete can be described using two-dimensional non-linear material FE models in a dynamic analysis. The models must include the material properties of the rock and the detonation. It is possible to follow the propagation of stress waves through the rock mass, from the centre of blasting to the reflection at the shotcrete-rock interface. The numerical simulation, conducted especially to study the influence of blast-creating, has demonstrated the reliability of the analysis compared with the acquired measurement from APSE tunnel. It is acceptable to use elastic material formulations for shotcrete since the blasting stress load does not exceed the elastic range. Responses of the shotcrete subjected to blasting vibrations with delay time are also presented. It is concluded that the consequences of the detonation of explosive points with a delay time of 1 ms causes a shorter rise time and a lower highest in the tensile stress at the interface. Therefore, from the view of tensile stresses at the shotcrete-rock interface, the vibration induced by delay time is less harmful to shotcrete than what was expected.

After the first phase of the project, the perspective has been widened to include fractured rock, which is represented as a translating wedge, i.e. a single rigid body. This has been possible since the analytical methods and models used have been possible to develop for both cases. By applying fractured rock areas, it is possible to study the protecting, filtering effect that the cracked rock volume has. Compared with shotcrete on intact rock, a stress reduction of about 70%, in the direction normal to the wall tunnel, can be noticed due to the filtering effect of the

fractured rock. While for the stresses in the direction parallel with the tunnel wall, there is no significant reduction in the stresses indicating that the shear stresses are predominate in this case.

Further study is required for the influence of the domination of shear stresses. The shear stress of shotcrete will be studied and compared with measurements that were conducted by Holmgren (1987), using punching block tests to estimate load applied on a shotcrete lining. For this further study, a paper has been prepared for the World Tunnelling Congress ITA-AITES (WTC) Tunnelling Conference 2017, where the results from laboratory tests on statically loaded bolt-anchored, steel-fibre-reinforced shotcrete linings in interaction with rock will be evaluated using a 2D finite element model. Calculations will be made to determine the state of stress in the shotcrete-rock interface near the rock joints. The simulated crack position and force-displacement curves will be compared with laboratory test results. The dynamic load cases are also analysed and compared to results from previous research on vibration resistance of shotcrete. Compared with the static load, this work will give a description of the dynamic behaviour of shotcrete on hard, jointed rock exposed to blasting.

Bibliography

Abaqus. (2014) Simulia: http://www.simulia.com/products/abaqus_explicit.html.

Ahmed L, Ansell A, Malm R. (2012b) Finite element simulation of shotcrete exposed to underground explosions. Nordic Concrete Research 45:59-74.

Ahmed L, Ansell A, Malm R. (2016) Numerical modelling and evaluation of laboratory tests with impact loaded young concrete prisms. Materials and Structures 49(11):4691–4704.

Ahmed L, Ansell A. (2012a) Laboratory investigation of stress waves in young shotcrete on rock. Magazine of Concrete Research 64(10):899-908.

Ahmed L, Ansell A. (2014) Vibration vulnerability of shotcrete on tunnel walls during construction blasting. Tunnelling and Underground Space Technology 42:105–11.

Ahmed L. (2012a) Laboratory simulation of blasting induced bond failure between rock and shotcrete. Stockholm: Rock Engineering Research Foundation. BeFo report 116.

Ahmed L. (2012b) Models for analysis of shotcrete on rock exposed to blasting. Licentiate thesis. Stockholm: KTH Royal Institute of Technology.

Ahmed L. (2015) Models for analysis of young cast and sprayed concrete subjected to impact-type loads. Doctorate thesis. Stockholm: KTH Royal Institute of Technology.

Andersson A. (2003) Aspö Pillar Stability Experiment. Summary of preparatory work and predictive modelling. SKB R-03-02, Svensk Kärnbränslehantering AB.

Ansell A. (1999) Dynamically loaded rock reinforcement. Doctoral thesis. Stockholm: KTH Royal Institute of Technology.

Ansell A. (2004) In situ testing of young shotcrete subjected to vibrations from blasting. Tunnelling and Underground Space Technology 19:587–596.

Ansell A. (2007) Dynamic finite element analysis of young shotcrete in rock tunnels. ACI Structural Journal 104(1):84-92.

Barrett S, McCreath D. (1995) Shotcrete support design in blocky ground: Towards a deterministic approach. Tunnelling and Underground Space Technology, 10, 79–89.

Bryne LE, Holmgren J, Ansell A. (2011) Experimental investigation of the bond strength between rock and hardening sprayed concrete. Proceedings of the Sixth International Symposium on Sprayed Concrete, Norwegian Concrete Society, Tromsø .

Bryne LE. (2014) Time dependent material properties of shotcrete. Doctoral thesis. Stockholm: KTH Royal Institute of Technology.

Dowding C H. (1996) Construction vibrations. Upper Saddle River, NJ: Prentice-Hall.

Hahn T, Holmgren J. (1979) Adhesion of shotcrete to various types of rock surfaces and its influence on the strengthening function of shotcrete when applied on hard jointed rock. In: Proceedings of the 4th International Congress on Rock Mechanics. Montreux: International Society for Rock Mechanics; 431–439.

Holmgren J. (1987) Bolt-anchored, steel- fiber-reinforced shotcrete linings. Tunnelling and Underground Space Technology, 2, 319–333.

Malmgren L, Nordlund E. (2008) Interaction of shotcrete with rock and rock bolts – A numerical study. International Journal of Rock Mechanics and Mining Sciences, 45, 538–553.

McCreath D R, Tannant D D, Langille C C. (1994) Survivability of shotcrete near blasts. In: Nelson PP, Laubach SE, editors. Rock Mechanics. Rotterdam, Balkema, 277–284.

Nakano N, 'Okada S, Furukawa K, Nakagawa K. (1993) Vibration and cracking of tunnel lining due to adjacent blasting (in Japanese, Abstract in English). Proceedings of the Japan Society of Civil Engineers, 3, 53–62.

Nyberg U, Harefjord L, Bergman B, Christiansson R. (2008) Monitoring of vibrations during blasting of the APSE.' SKB Report R-05-27, Sweden.

Ramana Y V, Gogte B S (1989) Dependence of coefficient of sliding friction in rocks on lithology and mineral characteristics. Engineering Geology 26: 271–279.

Reidarman L, Nyberg U. (2000) Blast vibrations in the Southern Link tunnel - Importance for fresh shotcrete? (in Swedish: Vibrationer bakom front vid tunneldrivning i Södra Länken - Betydelse för nysprutad betong?). Stockholm: Rock Engineering Research Foundation. SveBeFo-report 51.

Saiang D., Malmgren L., Nordlund E. (2005) Laboratory tests on shotcrete- rock joints in direct shear, tension and compression,' Rock Mechanics and Rock Engineering 38, 275–297.

Song K., Cho G. (2009) Bonding state evaluation of tunnel shotcrete applied onto hard rocks using the impact-echo method. NDT&E International Journal, 42, 487-500.

Song K., Cho G. (2010) Numerical study on the evaluation of tunnel shotcrete using the impact-echo method coupled with Fourier transform and shot-time Fourier transform. International Journal of Rock Mechanics & Mining Sciences, 47, 1274-1288.

Yang J H, Lu W B, Jiang Q H, Yao C, Zhou C B. (2016) Frequency comparison of blast-induced vibration per delay for the fullface millisecond delay blasting in underground opening excavation. Tunnelling and Underground Space Technology 51: 189-201.

BeFo

Box 5501
SE-114 85 Stockholm

info@befoonline.org • www.befoonline.org
Visiting address: Storgatan 19, Stockholm

ISSN 1104-1773